

Potential of *Aspergillus flavus* Secondary Metabolites in Breast Cancer Treatment In-silico Study of Fungal Compounds Targeting Tumor Suppressor Proteins

Shahad S. Alsharif¹, Bayan H. Sajer^{1,2,*} 

¹Department of Biological Sciences, King Abdulaziz University, Jeddah 80200, Saudi Arabia.

²Immunology Unit, King Fahd Medical Research Center, King Abdulaziz University, Jeddah, Saudi Arabia.

*Correspondence to: Bayan H. Sajer (E-mail: bsajer@kau.edu.sa)

(Submitted: 27 December 2024 – Revised version received: 05 January 2025 – Accepted: 03 February 2025 – Published online: 26 April 2025)

Abstract

Objectives: Breast cancer is one of the leading causes of mortality worldwide, with existing treatments often accompanied by significant side effects. This study aimed to explore the therapeutic potential of secondary metabolites derived from *Aspergillus flavus* in targeting key tumor suppressor proteins associated with breast cancer, namely BRCA1, BRCA2, and TP53.

Methods: An in-silico approach was employed to screen and evaluate fungal secondary metabolites. Molecular docking studies were conducted to assess the binding affinity of these compounds to BRCA1, BRCA2, and TP53 proteins. In addition, the pharmacological profiles of the compounds were analyzed, including ADME (absorption, distribution, metabolism, and excretion), cytotoxicity on cancer cell lines, and cardiotoxicity predictions.

Results: Among the analyzed secondary metabolites, vitexin demonstrated the highest binding affinity to BRCA1, BRCA2, and TP53, suggesting a strong potential for inhibiting these tumor suppressor proteins. The compound also showed favorable pharmacokinetic and safety profiles, indicating its suitability as a drug candidate.

Conclusion: Vitexin from *Aspergillus flavus* shows promise as a lead compound for the development of selective and effective inhibitors targeting tumor suppressor proteins involved in breast cancer. This study provides a foundational step toward designing safer and more targeted therapeutics using fungal-derived bioactive compounds.

Keywords: Molecular docking, Breast Neoplasms, Genes, Tumor Suppressor, Pharmaceutical Preparations

Introduction

Breast cancer (BC) has become globally the utmost frequent cancer, surpassing all other malignancies.¹ In Saudi Arabia, it is also the most prevailing cancer, with a significant increase in incidence over the past 15 years. It ranks as the second primary source of mortality in the country.²⁻⁴ According to data from the Saudi Cancer Registry, BC described for 14.2% of all cancer cases and 29% of cases in Saudi females in 2020.⁵

The ASR (age-standardized prevalence rate) for the female population was 28.8 per 100,000.⁶ Most BCs are sporadic (90–95%), while 5–10% can be accredited by genetic susceptibility, particularly in patients with a robust family history of the disorder.^{7,8} Hereditary breast cancers, which make up a large portion (about 80–90%) of cases, are associated with germline mutations in the breast tumor suppressor gene 1 (BRCA1), Breast tumor suppressor gene 2 (BRCA2), and Tumor protein-53 (TP53) genes.⁹ BRCA2 and BRCA1 are human tumor suppressor genes responsible for regulating DNA repair, transcriptional activation, apoptosis, cell-cycle checkpoint regulation, and chromosomal remodeling.^{10,11} When a BRCA1 or BRCA2 mutation occurs, DNA repair is impaired, leading to an increased threat of breast cancer.^{12,13} Currently, BRCA2 and BRCA1 are considered the most significant “high-risk” genes, accounting for numerous issues of breast and ovarian cancer within families.¹⁴ The TP53 gene functions as a tumor suppressor by regulating cell growth and division, safeguarding cells from DNA damage-induced genome alterations by inhibiting proliferation or inducing apoptosis.¹⁵ Despite significant progress, conventional treatments for breast cancer (BC) including chemotherapy, radiation, and hormone therapies—still face critical limitations such as drug resistance, off-target

toxicity, and recurrence.¹⁶ These issues highlight the need for novel, less toxic, and more targeted therapeutic options.

Natural sources have long been essential in drug discovery, with nearly 60% of anticancer drugs derived from natural products.¹⁷ Among them, fungi have gained increasing attention for their ability to produce structurally diverse and biologically active secondary metabolites with relatively low toxicity to normal cells.¹⁸ *Aspergillus flavus*, in particular, is known to produce several bioactive compounds with therapeutic potential, including vitexin, ergonovine, triterpenoids, luteolin, and phytosterols. The antimicrobial and antioxidant activities of *A. flavus* are largely attributed to its rich phenolic and flavonoid content.¹⁹⁻²¹

Fungal metabolites encompass a wide range of chemical classes—such as alkaloids, macrolides, terpenes, and anthra-cenones—and over 148,000 have been identified to date. Several compounds, including gliotoxin, chaetocin, and cordycepin, have demonstrated promising anti-breast cancer activity in both in vitro and in vivo studies, further supporting fungi as a promising platform for anticancer drug development.²²

However, despite their promising anticancer activities, the full potential of fungal metabolites—especially from *A. flavus*—has not been fully explored in breast cancer therapy, particularly through computational methods. This research gap presents an opportunity to uncover novel therapeutic agents.

To accelerate the identification of such compounds, computational methods like molecular docking have become widely used. These techniques help predict interactions between small molecules and biological targets, enabling the efficient screening of large compound libraries.^{19,23} Docking also supports the design of selective and potent drug candidates by

revealing binding affinities and preferred molecular orientations.^{23,24} This is especially valuable in oncology, where understanding drug-target interactions can lead to more effective therapies with fewer side effects.²⁵

Therefore, the objective of this study is to systematically evaluate selected fungal metabolites—previously identified for their anticancer properties—for their capacity to interact with key proteins implicated in breast cancer progression, employing advanced in silico methodologies. The aim is to identify novel, targeted therapeutic candidates that exhibit enhanced specificity and reduced toxicity.

Materials and Methods

The computational software applied for this experiment contains AutoDockTools (v. 1.5.7), Discovery Studio (v.21.1.0.0), and other online computational devices accessible. This work did not require ethical approval as all data used in this study were extracted from websites. The selection of three secondary metabolites from the fungus *A. flavus* was reported in a recently published literature against breast cancer. The secondary metabolites selected include vitexin, beta-carotene, and ferulic acid.

Selection and Preparation of Ligands

Three secondary metabolites from a fungal source were reported in a previous study as highly effective compounds with anticancer potential.¹⁹ Secondary metabolites were collected and downloaded from a public database (<https://pubchem.ncbi.nlm.nih.gov>) in SDF format **Figure 1**. The chemical structure of the screened compounds used in this study; (**Fig. 1a**) Vitexin (**Fig. 1b**) Beta-carotene (**Fig. 1c**) Ferulic acid and (**Fig. 1d**) Tamoxifen. The ligands were converted to PDB format using the software Open Babel (http://openbabel.org/wiki/Main_Page) to prepare them for docking exploration. AutoDockTools was used to add hydrogen atoms to the ligand molecules, set root and torsions. The ligand was saved in PDBQT file format.

Proteins Collection and Preparation

The 3D-structures of target proteins BRCA1 (PDB ID: 3PXE), BRCA2 (PDB ID: 1T38), and TP53 (PDB ID:7L1O) were

obtained from Protein Databank (<https://rcsb.org/>) in PDB format **Figure 2**. The structures were assessed for the presence of missing residues and gaps using PyMol, water molecules and unnecessary chains were removed from the structure. The proteins with missing residues were remodeled using Swiss-Modeller. The structures were refined using GalaxyRefine and best models were evaluated on the basis of maximum favored residues in Ramachandran Plot. High molprobit score, low clash score and poor rotamers, low RMSD with original structure and high GDT-HA score estimated by GalaxyRefine. The refined structures were further assessed in AutoDockTools for presence missing atoms. The missing atoms were repaired using Repair Missing Atom Wizard of AutoDockTools. Polar hydrogen atoms were added to the structure and overall charge of protein was balanced by adding Kollman charges. The protein structure was saved in PDBQT format for further steps.

Receptor Grid Preparation and Molecular Docking

The prepared protein structures were analyzed using PrankWeb server to identify binding pockets. The best binding

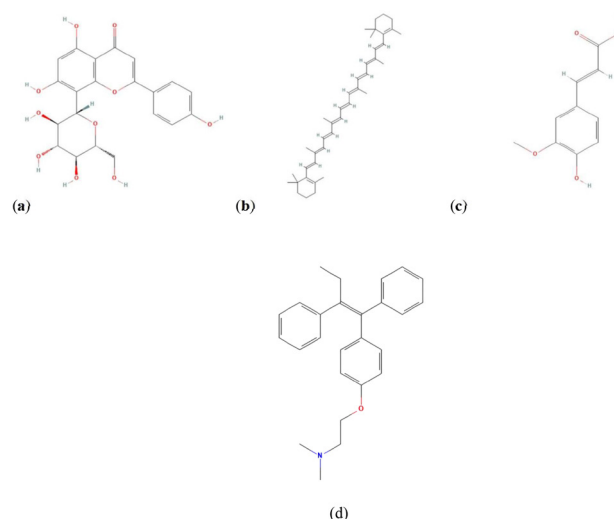


Fig. 1 The chemical structure of the screened bioactive molecules used in this study; (a) Vitexin (b) Beta-carotene (c) Ferulic acid and (d) Tamoxifen.

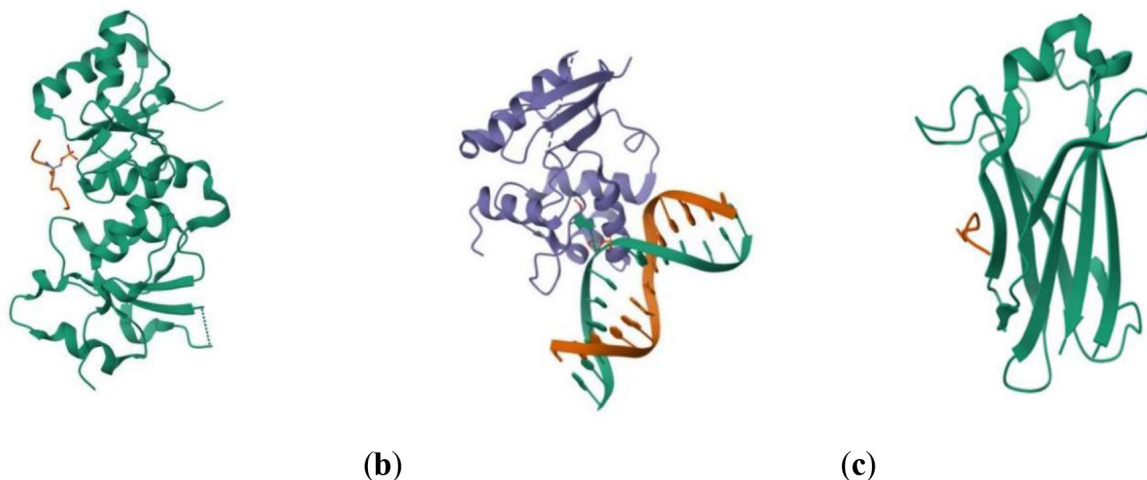


Fig. 2 The three-dimensional structure of (a) BRCA1 (3PXE), (b) BRCA2 (1T38), and (c) TP53(7L1O).

pocket was selected on the basis of pocket size and volume. A grid box of 60 X 60 X 60 was used along with spacing range of 0.303 – 0.503 Å (Table 1). The ligand interaction maps were generated using AutoGrid4. Molecular docking simulation was performed using Lamarckian Genetic Algorithm. A docking parameter file was generated for Number of GA Runs: 100, Population Size: 150, Rate of Gene Mutation: 0.02. The docking was executed using AutoDock4. AutoDock4 performed a clustering of best binding poses and ranked them on the basis of total binding energies. The docked poses having highest binding affinities were retrieved from the docking log file generated by AutoDock4. The non-bonding interaction of best docked pose with target proteins was visualized in 2D and 3D form using BIOVIA Discovery Studio. The reliability of the docking methodology was validated through re-docking (self-docking) of bioactive compounds with the target proteins used throughout the investigation.

Investigation of the Compounds for Lipinski's Rule of Five (RO5)

Lipinski's Rule of Five (RO5) is utilized to assess the drug-likeness of a compound. The molecular actions and drug-likeness of the biological molecules were analyzed based on RO5. This rule, developed by Christopher A. Lipinski in 1997, serves as a guideline for evaluating drug likeness by considering parameters such as molecular weight, lipophilicity, hydrogen acceptor, hydrogen donor, and molar refractivity.^{26,27} In this work, ligands were showed for RO5 conformity using the Supercomputing facility for computational and bioinformatics biology (<http://www.scfbio-iitd.res.in/software/drugdesign/lipinski.jsp>).

Physicochemical and ADME Properties

The ADME (Adsorption, Distribution, Metabolism, and Excretion) and physicochemical analyses were conducted to determine the pharmacodynamic properties of the molecule. The ADME evaluation of the chosen potential compounds was performed using the pkCSM platform and SwissADME (<http://www.swissadme.ch/index.php>). For physicochemical activities, only SwissADME was utilized. This assay aims to provide valuable insights for drug research and development.²⁸ The assessment was conducted for each physicochemical property and ADME by presenting a SMILE format of the single molecule acquired from the PubChem database. The investigation was established on a comprehensive database containing 288,967 attempts from peer-reviewed publications, EPA, ChEMBL, and DrugBank databases. For ADME properties, all the files were confirmed and handled using the Molecular Operating Environment (MOE, version 2016). The properties were divided into 6 modules (basic, A, D, M, and E) and a sequences of subclasses based on their endpoint implications.²⁹

Assessment of Blockage of hERG K⁺ Channels

The human ether-à-go-go-related gene (hERG) encodes the subunit of a voltage-gated K⁺ channel that acts as a delayed rectifier, crucial for cardiac action potential repolarization.³⁰ Dysfunction of the hERG gene,³¹ can lead to substantial delays in heartbeats, potentially resulting in sudden death.³⁰ Computational methods are increasingly used for rapid and cost-effective assessment of chemical compounds. The Pred-hERG 5.0 web server is a valuable tool for evaluating the toxicity of metabolites by assessing hERG K⁺ channel blockage. This web server utilizes advanced machine learning models to predict hERG blockage accurately, with an expanded database, meticulous data curation, diverse prediction models, and improved accuracy. It offers a user-friendly interface for drawing chemical structures, uploading compound files, initiating evaluations, and reviewing results. Pred-hERG 5.0 is essential for assessing compound cardiotoxicity, a requirement in US FDA clinical trials.³² The results are stated as probability forecasts, distinguishing between compounds that block and those that do not block the hERG channel. A confidence value not exceeding 0.26 indicates a non-cardiotoxic compound.³³ The segments that depict hERG inhibition can be seen on the probability map.

We used the cardioTox CAM web server, a computational platform designed for assessing cardiotoxicity. This platform can accurately predict six common clinical cardiac toxicity outcomes: hERG toxicity, heart block, cardiac failure, myocardial infarction, arrhythmia, and hypertension. Furthermore, it can identify substructures that are supplemented in toxic constituents, delivering validation for explanation and further evaluation.³⁴

Prediction of Cell Line Cytotoxicity

Cytotoxicity prediction is achieved using the freely available online tool CLC-Pred 2.0 (Cell Line Cytotoxicity Predictor).³⁵ An accessible online tool called PASS CLC Pred has been developed to forecast the cytotoxicity of chemicals against tumor and normal human cell lines from various tissues using the mentioned PASS models. (<http://www.way2drug.com/Cell-line/>).³⁶ PASS has the capability to predict around 4000 different biological activities, including machineries of action, toxic and adverse properties, interactions with metabolic enzymes and transporters, as well as pharmacological consequences on transcriptomic analysis.³⁷ The molecular structures of Vitexin, beta-carotene, and Ferulic acid were submitted in SMILES format. The resulting data was shown as activation probability (Pa) and inactivation probability (Pi) values.³⁸ These values can range from 0.000 to 1.000.³⁹ When Pa > Pi, a specific compound is deemed to exhibit potential activity. The pharmacological action is deemed strong when Pa > 0.7 and weak when 0.5 < Pa < 0.7.⁴⁰ Data can be pulled out in a structured data file format. The analysis of data obtained

Table 1. The results of estimated inhibition constant, Ki using an AutoDock tool software

Protein	Ki of Functional group 1 (vitexin)	Ki of Functional group 2 (beta-carotene)	Ki of Functional group 3 (ferulic acid)	Ki of Functional group 4 Tamoxifen
BRCA1 (3PXE)	109.07 nM	870.08 nM	4700.00 nM	44760.00 nM
BRCA2 (1T38)	140.61 nM	860.61 nM	401.62 nM	950.09 nM
TP53 (7LIO)	278.43 nM	7420.00 nM	11570.00 nM	51700.00 nM

Ki, Estimated Inhibition Constant; nM = nanomolar.

from CLC-Pred is interpreted according to their IC₅₀ (half maximal inhibitory concentration), IG₅₀ (half-maximal inhibitory growth), and % inhibition (of activity) values. Molecules are deemed active if they exhibit inhibition greater than 50% with IG₅₀ and IC₅₀ values of 10,000 nM.⁴⁰

Results and Discussion

Molecular Docking Analysis

Molecular docking is a fundamental technique to virtually predict strong binders and screen a library of potential molecules. Given that tumor suppressor genes contribute to cancer development when inactivated or lost, there is a critical need to develop appropriate drug candidates that can effectively inhibit tumor growth with minimal adverse effects.

The binding affinity between receptors and ligands is determined by binding energy—lower energy values indicate higher binding affinity. In this study, three secondary metabolites were screened against BRCA1/3PXE, BRCA2/1T38, and TP53/7LIO protein targets. Following the docking process, we analyzed and recorded several parameters as shown in Table 1, including inhibitory constants binding energy (kcal/mol), number of hydrogen bonds formed, and the specific amino acid residues involved in these interactions.

The secondary metabolites, vitexin, beta-carotene, and ferulic acid demonstrated notable binding affinities against key cancer-related receptors. Against BRCA1 (PDB ID: 3PXE), these compounds exhibited binding energies of -9.5, -8.27, and -7.27 kcal/mol, respectively. Similarly, their interaction with BRCA2 (PDB ID: 1T38) resulted in binding energies of -9.35, -8.27, and -8.73 kcal/mol. In the case of TP53 (PDB ID: 7LIO), vitexin, beta-carotene, and ferulic acid showed binding energies of -8.94, -7.00, and -6.73 kcal/mol, respectively.

When compared with the reference ligand, all three compounds—particularly vitexin—exhibited superior binding affinities across all three receptors, as detailed in Table 2.

Table 2. The results of docking for some secondary metabolite against BRCA1, BRCA2, and TP53 proteins

Compounds	BRCA1 (3PXE)	BRCA2 (1T38)	TP53 (7LIO)
Vitexin	-9.5	-9.35	-8.94*
Beta-carotene	-8.27	-8.27	-7.0
Ferulic acid	-7.27	-8.73	-6.73
Tamoxifen	-5.93	-8.22	-5.85

*The unit of binding energy = kcal/mol.

Table 3. Docking consequences for the best binding affinity with BRCA1 (3PXE) protein for three selected molecules

Drug	Binding affinity (kcal/mol)	No. of H-bond	Residues amino acids
Vitexin	-9.5	4	Ala1693, Phe1695, Phe1734, Asp1733, His1732, Glu1735
Beta-carotene	-8.27	0	Lys1759, Arg1762, Arg1758, Ser1755, Arg1751, Glu1754, Asp1757, Tyr1845, Gln1846, Ile1760, Cys1847, Ile1807, Leu1764, Pro1806, Leu1850, His1805, Pro1831
Ferulic acid	-7.27	3	Glu1694, Phe1695, Arg1737, Asp1733, Phe1734, His1732, Glu1735, Arg1753, Val1736, Gln1747, Lys1750
Tamoxifen*	-5.93	1	Thr1700, Ser1655, Gly1656, Val1654, Leu1701, Leu1705, Ile1680, Lys1702, Leu1657, Phe1662, Leu1679

* = Reference ligand.

Interaction and Binding Affinity of Compounds

Herein, the interactions, hydrogen bonds, and residues of amino acids were calculated using Autodocktools 4.2.6 and Discovery Studio Software for generating a 2D structure. For the BRCA1 (3PXE) protein, vitexin showed the highest binding energy compared to the other derivatives, exhibiting a binding affinity of -9.5 kcal/mol Table 3. The compound vitexin showed strong hydrogen bonding with Ala1693, Glu1735, and His1732, and exhibited one pi-pi bond with Phe1695, and Phe1734 Figure 3. In addition, beta-carotene exhibited van der Waals interactions with Glu1754, Asp1757, Arg1751, Ser1755, Asp1757, Tyr1845, Gln1846, Lys1759, Arg1762, Ile1760, Ile1807, and Pro1806; for amino acids that participated in Alkyl bonds, they were Arg1758, Cys1847, Leu1764, Pro1831, His1805, and Leu1850 Figure 4. The ferulic acid compound showed several van der Waals bonds with Phe1695, Asp1733, Phe1734, His1732, and Arg1753 Figure 5, also exhibited one carbon-hydrogen bond with Val1736, as well as Alkyl interactions with Lys1750. The reference ligand Tamoxifen showed one hydrogen bond with Gly1656, and pi cation with Lys1702, pi Alkyl bonds with Val1654, and Leu1701 Figure 6. The 2D and 3D structures of molecular interactions are presented in Figures 3–6.

Interaction and Binding Affinity of Compounds

The compounds vitexin, beta-carotene, and ferulic acid showed high binding results towards the BRCA2 (1T38) protein, with binding energies of -9.35, -8.27, and -8.73 kcal/mol, respectively Table 4. In the vitexin compound, we identified four strong hydrogen bonds with Ala83, Val81, Phe89, and Trp100, as well as a Pi-Alkyl bond with Leu84 Figure 7. Additionally, there were van der Waals interactions with Gln90, Arg96, Lys104, Lys101, Leu99, Leu103, and Pro82. Beta-carotene exhibited five hydrophobic interactions (alkyl and pi-alkyl bonds) with Trp65, Ile76, Kys107, Leu103, and Lys104, along with a Pi-sigma bond with Trp100 Figure 8. Van der Waals interactions were observed with Pro144, Val106, Arg147, Phe108, Glu77, Val81, Kys101, Glu92, Gln97, and Arg96.

In Ferulic acid, three hydrogen bonds were identified with Leu33, Asn137, and Tyr114, as well as an unfavorable sump with Lys165 Figure 9. Alkyl and pi-alkyl bonds were formed with Met134, and a Pi-sigma bond with Tyr158. Van der Waals interactions were observed with Pro140, Ser145, Ser159, Arg135, Ser145, Gly131, Asn157, and Val148. The drug tamoxifen exhibited two hydrogen bond with Asn137 and Tyr114, and pi sigma with Tyr158, Alkyl with Met134, Tyr114, van der waals with Val148 Figure 10. The 2D and 3D structures of molecular interactions are depicted in Figures 7–10.

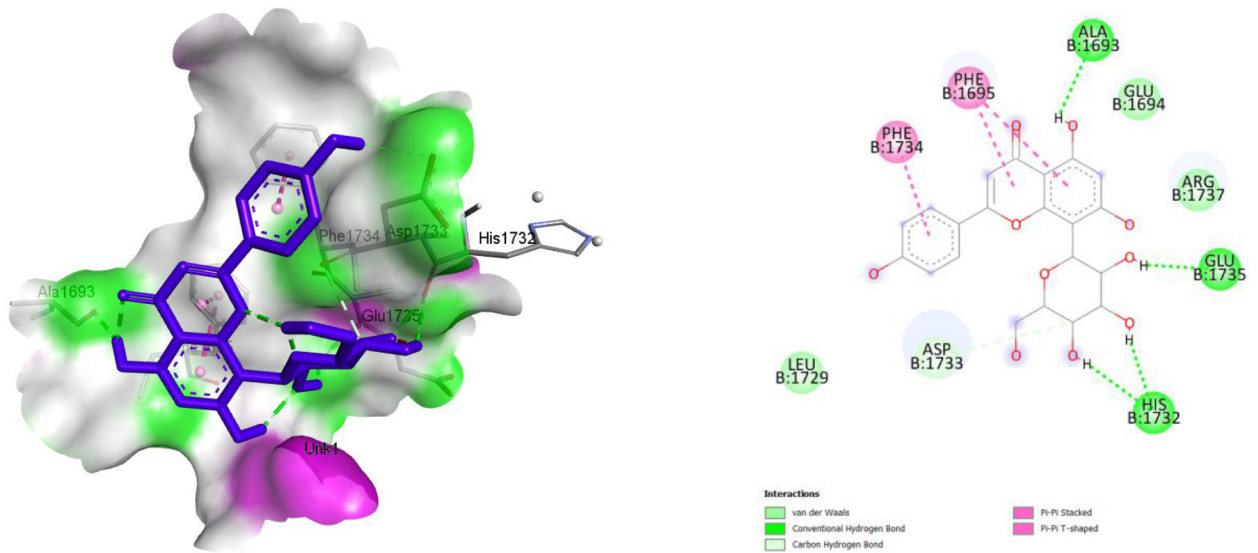


Fig. 3 The molecular interaction BRCA1 (3PXE) and Vitexin.

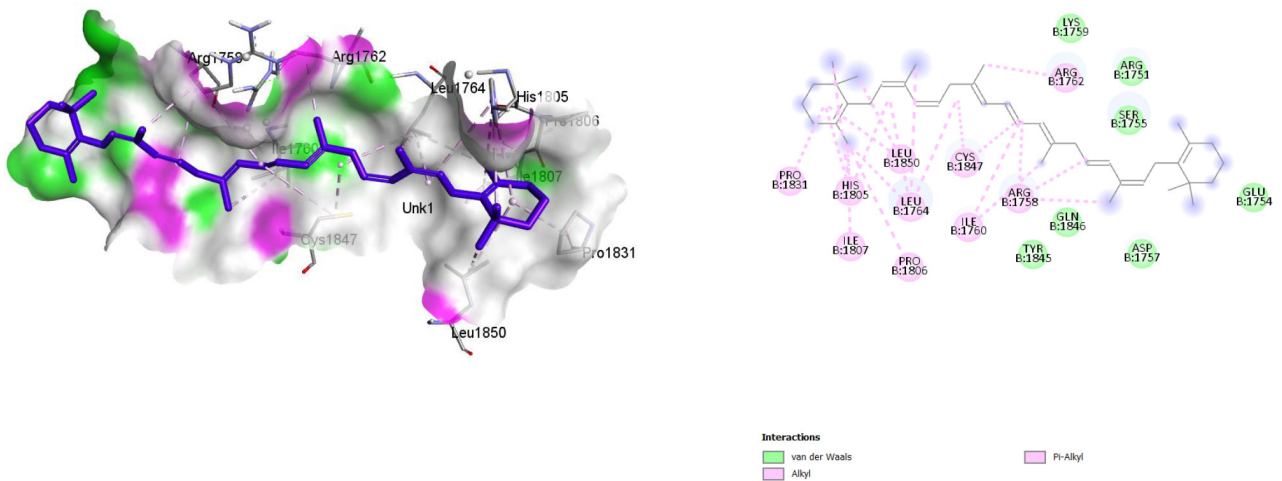


Fig. 4 The molecular interaction BRCA1 (3PXE) and beta-carotene.

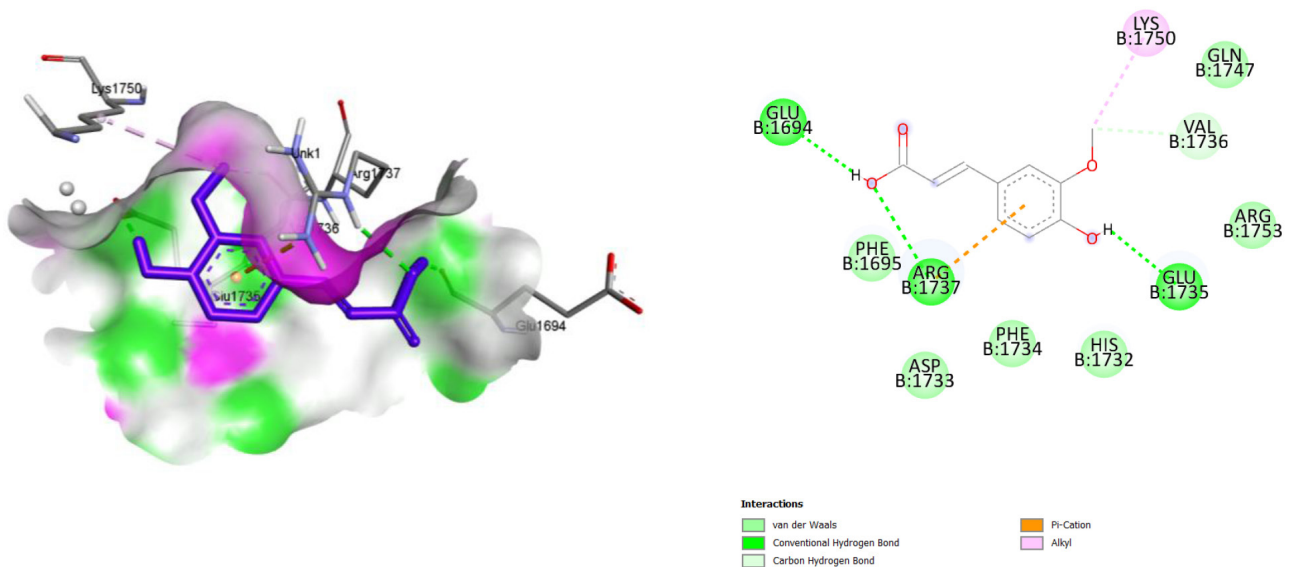


Fig. 5 The molecular interaction BRCA1 (3PXE) and ferulic acid.

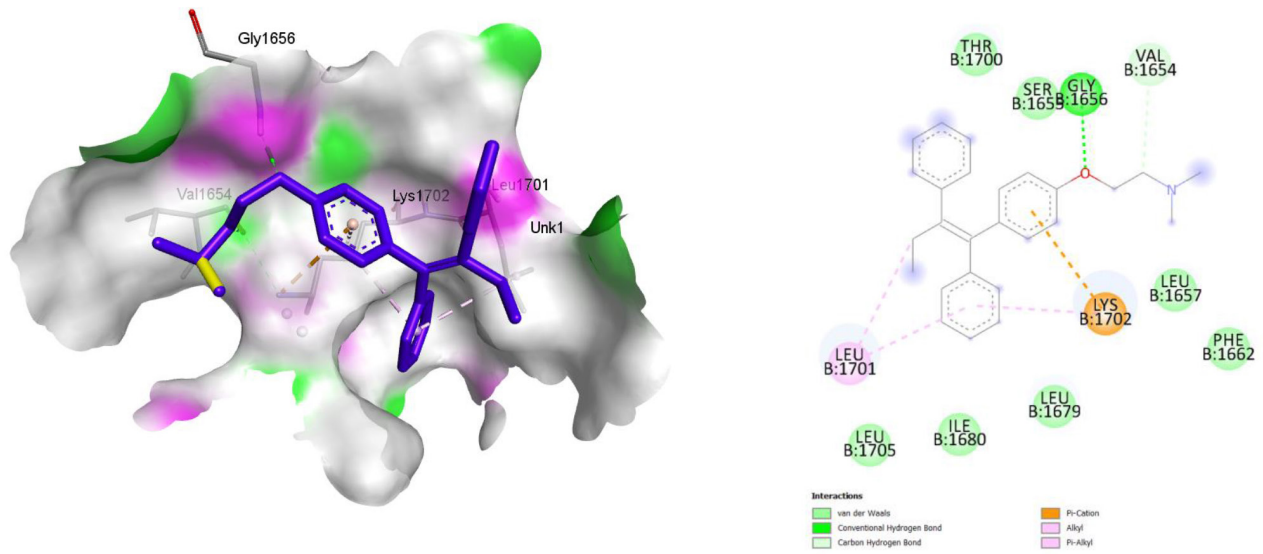


Fig. 6 The molecular interaction BRCA1 (3PXE) and Tamoxifen.

Table 4. The results of docking analysis for best binding affinity with BRCA2 (1T38) protein for three selected biomolecules

Drug	Binding affinity (kcal/mol)	No. of H-bond	Residues amino acids
Vitexin	-9.35	4	Ala83, Val81, Pro82, Leu84, Phe89, Gln90, Arg96, Lys104, Trp100, Lys101, Leu99, Leu103
Beta-carotene	-8.27	0	Glu92, Arp100, Pro144, Val106, Trp65, Ile76, Arg147, Lys107, Phe108, Glu77, Val81, Phe79, Leu103, Lys104, Lys101, Gln97, Arg96, Trp100.
Ferulic acid	-8.73	2	Leu33, Pro140, Ser145, Val148, Lys165, Asn157, Tyr114, Gly131, Met134, Arg135, Tyr158, Ser159, Asn137
Tamoxifen	-8.22	2	Leu33, Pro140, Ser145, Asn137, Ser159, Arg135, Tyr158, Met134, Val148, Lys165, Asn157, Tyr114, Gly131

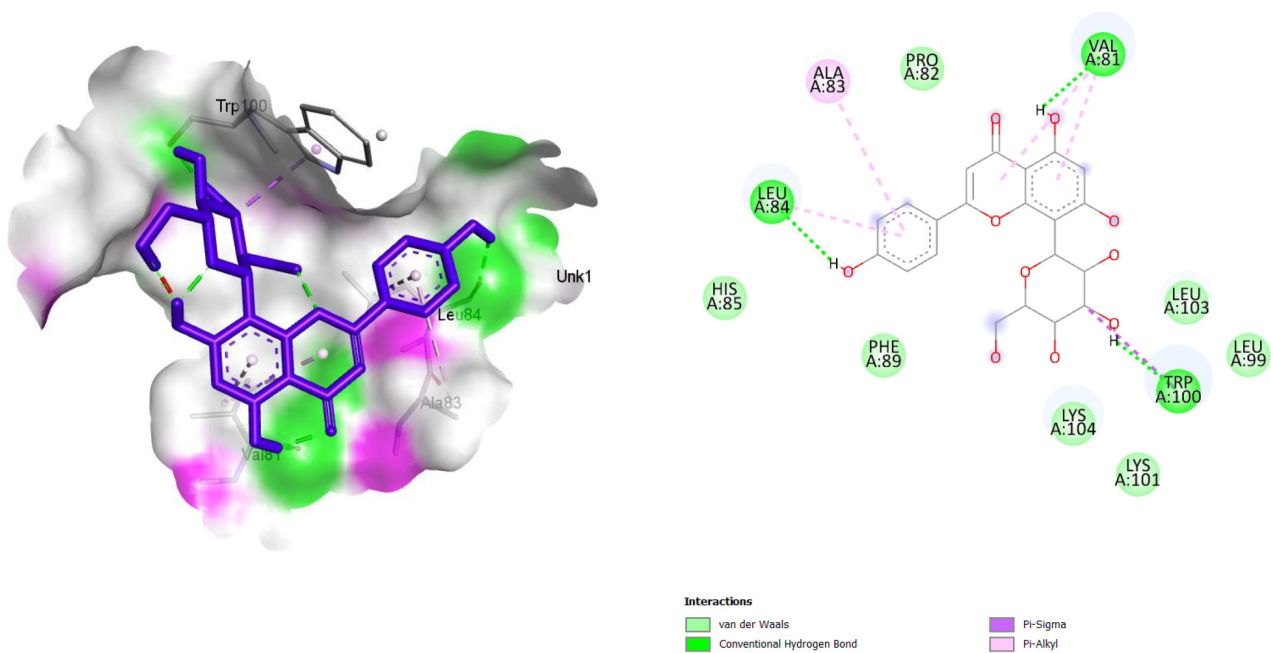


Fig. 7 The molecular interaction BRCA2 (1T38) and Vitexin.

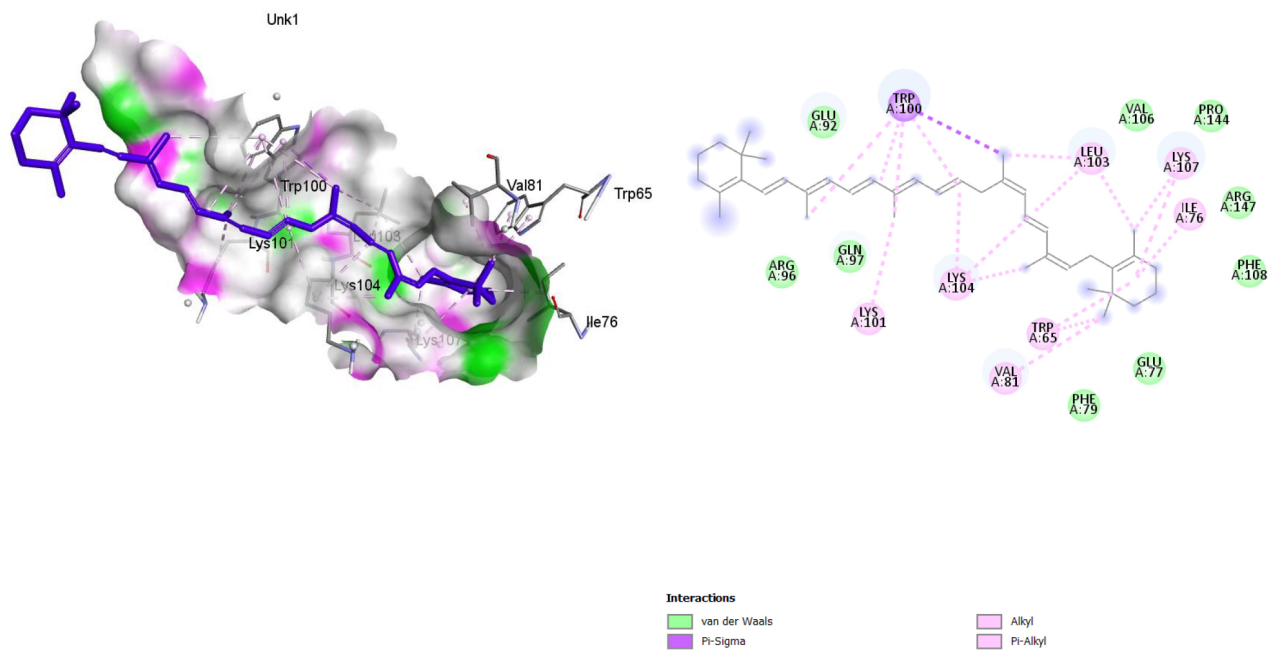


Fig. 8 The molecular interaction BRCA2 (1T38) and beta-carotene.

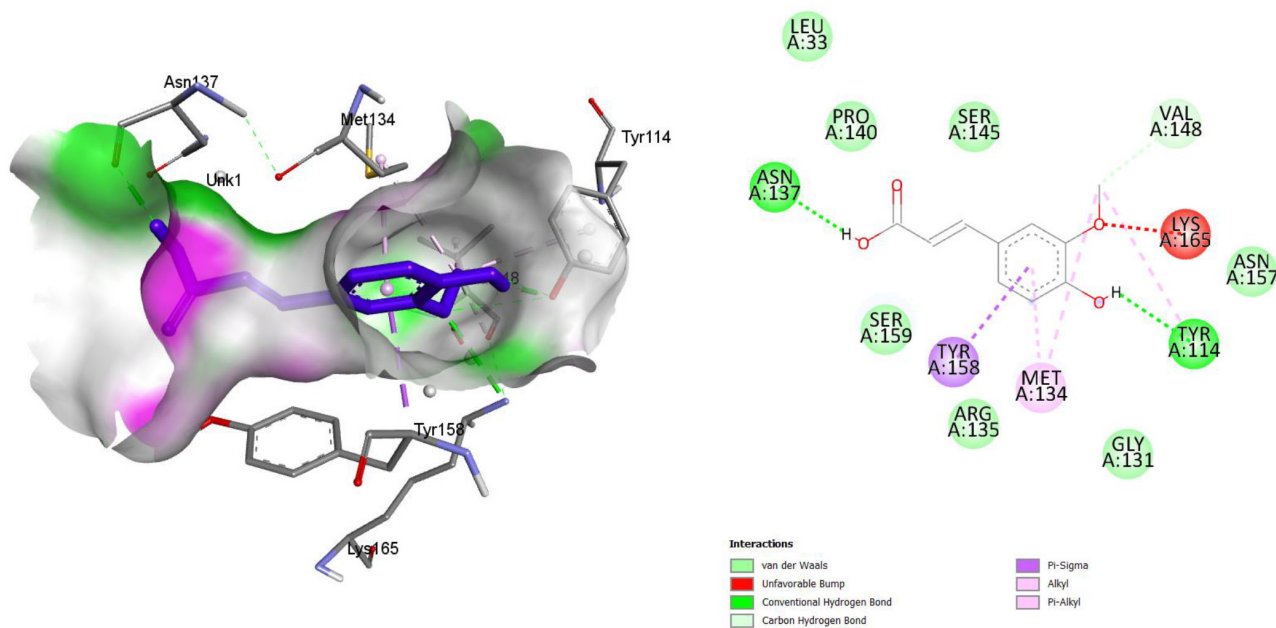


Fig. 9 The molecular interaction BRCA2 (1T38) and ferulic acid.

Interaction and Binding Affinity of Biomolecules

Among the compounds tested, vitexin showed significantly improved binding energy towards the TP53 (7LIO) protein compared to the other compounds. Vitexin formed strong hydrogen bonds with Thr56, Ser33, and Ser58, as well as one Pi-Pi interaction with Tyr34 Figure 11 and Table 5. On the other hand, beta-carotene formed several Pi-alkyl interactions with Leu150, Ala109, Lys110, and one Pi-sigma interaction with Phe43 Figure 12. Ferulic Acid exhibited a Carbon-hydrogen bond with Glu97 and Leu65, one Pi-sigma interaction with Val98, van der Waals interactions with Val30,

Arg99, Arg124, and Ser59, and one hydrogen bond with Val164 Figure 13. Additionally, there were Pi-alkyl interactions with Lys64, Pro94, Lys95, Val163, and Val163. The drug tamoxifen formed two carbon hydrogen bond with Lys135, pi anion with Lys134, pi Alkyl with Trp131, Tyr123, and pi-pi-T-shaped with Phe133 Figure 14. The 2D and 3D structures of molecular interactions are presented in Figures 11–14.

After conducting multiple docking simulations, the interaction of the ligand with the protein was analyzed. It was found that among the secondary metabolites tested, vitexin and beta-carotene exhibited the strongest binding interactions

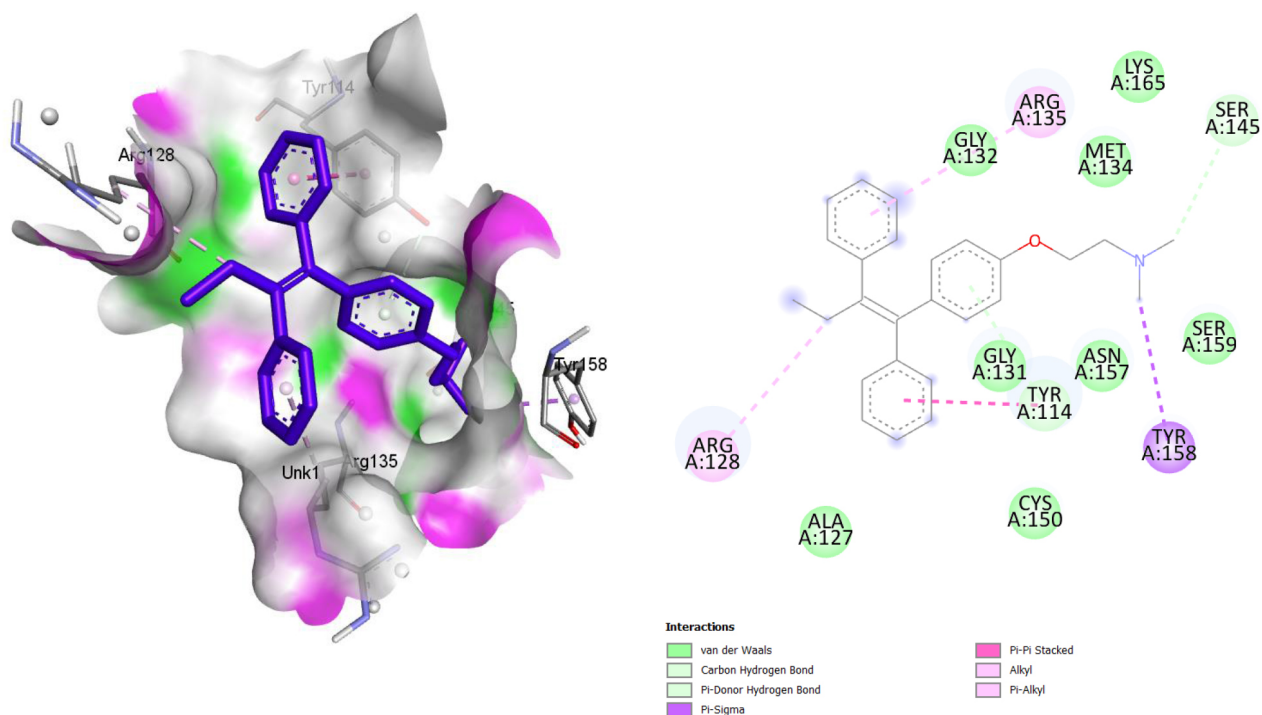


Fig. 10 The molecular interaction BRCA2 (1T38) and Tamoxifen.

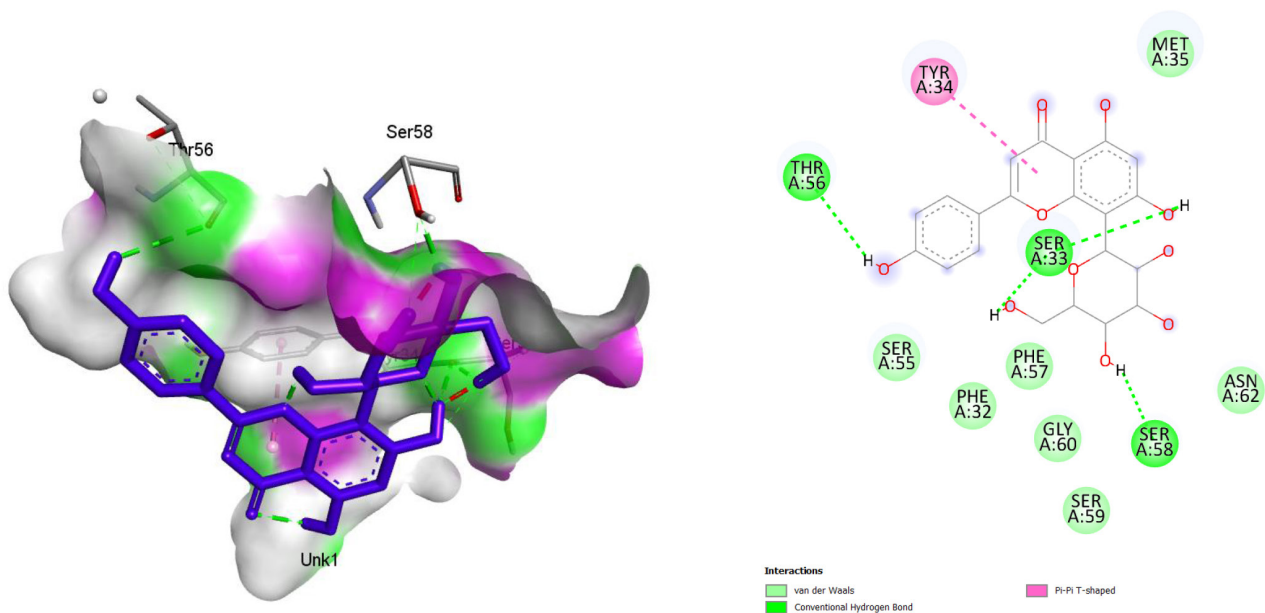


Fig. 11 The molecular interaction TP53 (7L10) and Vitexin.

Table 5. Docking results for best binding affinity with TP53 (7L10) protein for three compounds

Drug	Binding affinity (kcal/mol)	No. of H-bond	Residues Amino Acids
Vitexin	-8.94	4	Tyr34, Thr56, Ser33, Ser58
Beta-carotene	-7.0	0	Leu150, Ala109, Lys110, Phe43
Ferulic acid	-6.73	2	Val30, Trp67, Leu65, Lys64, Pro94, Ser59, Lys95, Val163, Val164, Arg99, Arg124, Glu97, Val98
Tamoxifen	-5.85	0	Asp119, Gly132, Phe102, Tyr87, Trp131, Tyr123, Phe133, Lys134, Lys135, Met117

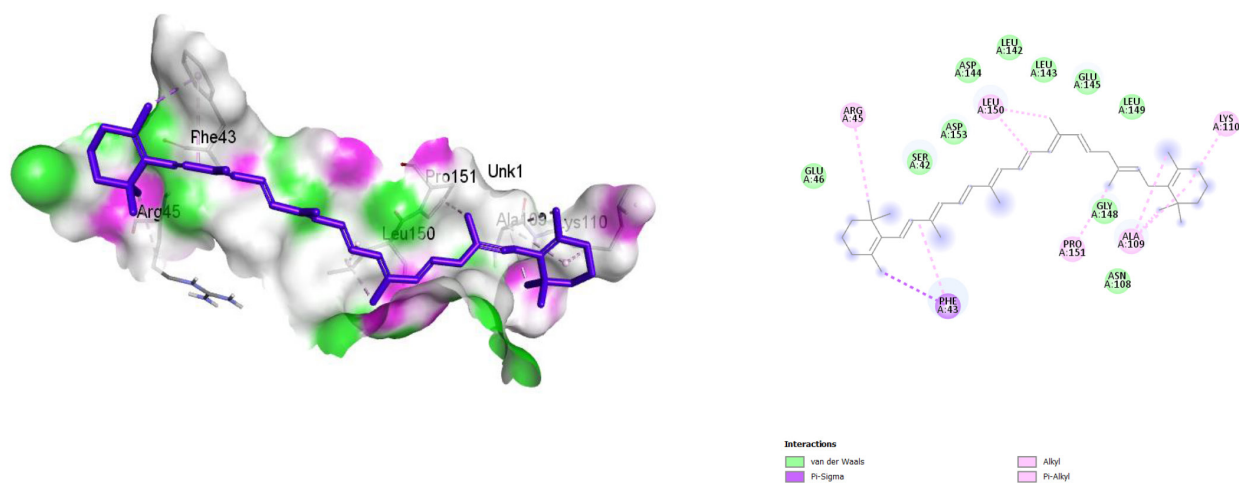


Fig. 12 The molecular interaction TP53 (7L10) and beta-carotene.

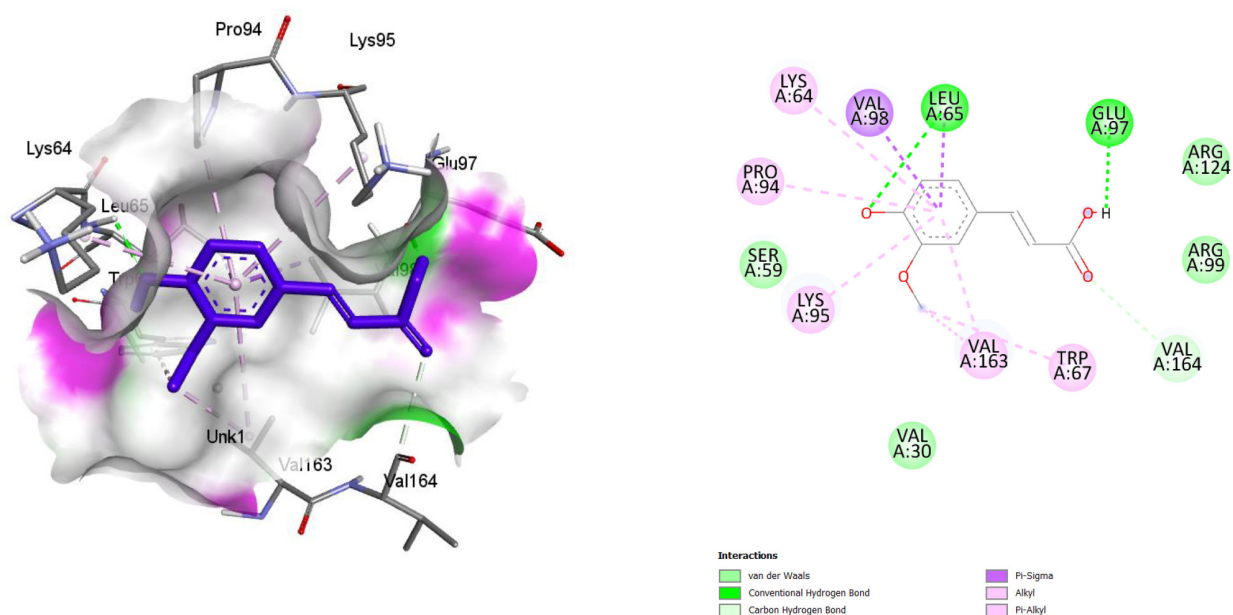


Fig. 13 The molecular interaction TP53 (7L10) and Ferulic Acid.

with all three proteins: BRCA1, BRCA2, and TP53. This discovery could be valuable for identifying and developing new preventive and therapeutic drugs for breast cancer.

Lipinski's Rule of Five (RO5) Analysis

Lipinski's Rule of Five, also known as Pfizer's Rule, is a method used to assess the drug-like properties of a biological molecule. This rule helps determine if a chemical compound influences specific biological actions or pharmacological properties that could potentially make it an applicable oral drug in humans.⁴¹ One crucial stage in drug discovery involves evaluating whether a particular compound is likely to be effective when taken orally. Lipinski's rule outlines the criteria for oral activity, stating that a drug should not violate more than one of the following conditions: molecular mass not exceeding 500 Daltons, a Log *P* value below 5 indicating limited lipophilicity, no more than 5 hydrogen bond donors, no more than 10 hydrogen bond acceptors, and a molar refractivity falling within the

range of 40–130.⁴² The data stated in Table 6 show that Ferulic Acid satisfied all five Lipinski criteria, while beta-carotene did not meet the criteria. Vitexin, however, only deviated from one of the criteria, which is considered acceptable. In addition, Tamoxifen was used as a reference ligand and fulfilled all the Lipinski parameters, further supporting its suitability as an orally active compound. Lipinski's rule suggests that an orally active drug should generally not violate more than one of the specified criteria.

Physicochemical and ADME Analysis

After the drug is administered to the human body or an animal model via any route, it undergoes ADME processes, leading to its active or passive transport to the target site.⁴³ When interacting with specific biological macromolecules, there can be both positive and negative pharmacological outcomes. The efficacy of a drug and its ability to reach the intended target in the body are influenced by its safety and efficacy. The primary

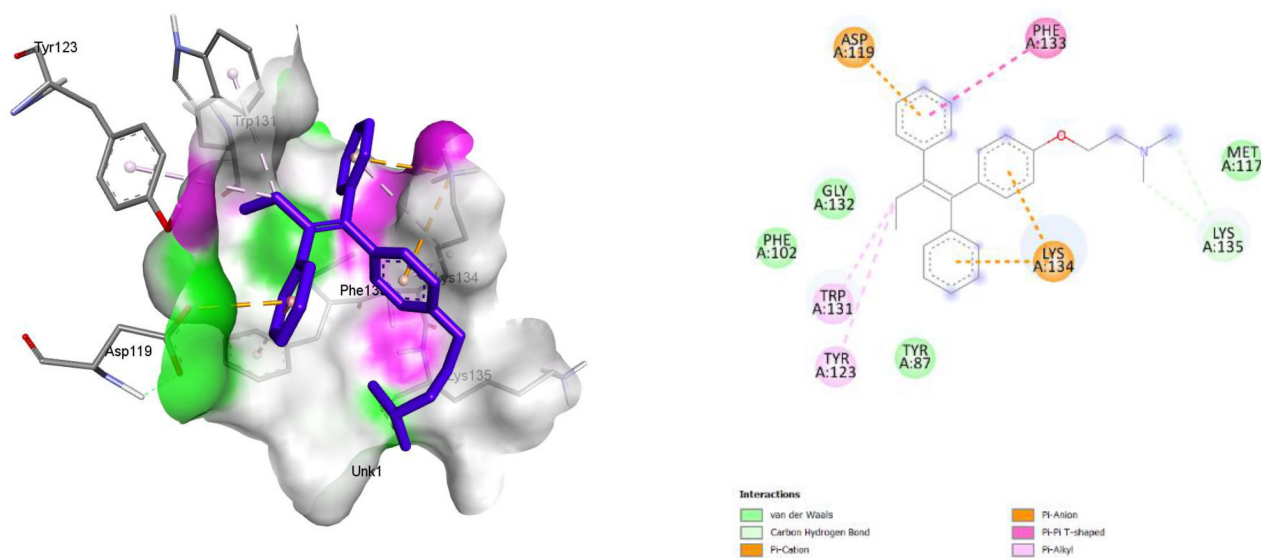


Fig. 14 The molecular interaction TP53 (7L10) and Tamoxifen.

Table 6. Lipinski's rule of 5, of the selected biomolecules used in this study

Secondary metabolite	Mass	Hydrogen bond donor	Hydrogen bond acceptor	LOG P	Molar refractivity
Vitexin	432	7	10	-0.065500	103.534050
Beta- carotene	536	0	0	12.605807	181.392334
Ferulic acid	194	2	4	1.498600	51.328594
Tamoxifen	342	0	1	1.562060	88.894981

reason for the failure of a drug is often its inadequate safety and efficacy, which is closely linked to its ADME properties. In this study, the ADME properties of three selected compounds were assessed using different *in silico* tools such as the SwissADME server, pkCSM server, and GUSAR. These evaluations aimed to gauge the pharmacokinetic properties, including lipophilicity, water-solubility, drug-likeness, medicinal chemistry, and toxicity of the compounds.⁴⁴ The compounds' lipophilicity enables them to readily pass through the cell membrane, making oral preparation unsuitable. Furthermore, an injectable dosage form might be a more favorable choice to attain a swift onset of action due to low gastrointestinal absorption. The physicochemical and ADME actions of the chosen compounds are detailed in Tables 7 and 8.

The physicochemical profiles of the selected compounds are summarized in Table 7. Ferulic acid exhibited the lowest molecular weight (194.18 g/mol) and moderate lipophilicity, while beta-carotene showed the highest lipophilicity across all log *P* models. Vitexin presented the highest TPSA (181.05 Å²), suggesting low membrane permeability, whereas beta-carotene showed no hydrogen bonding capabilities.

As presented in Table 8, all compounds demonstrated acceptable gastrointestinal (GI) absorption, with beta-carotene and Tamoxifen exceeding 90%. Blood-brain barrier (BBB) permeability was positive only for beta-carotene and Tamoxifen. Water solubility was lowest for beta-carotene, indicating poor aqueous solubility. In terms of metabolism, all compounds were predicted to be non-inhibitors of major CYP450 enzymes. Total clearance rates varied, with beta-carotene showing the highest predicted excretion rate.

Bioavailability Radar

The bioavailability radar quickly evaluates the compound's suitability as a drug. The pink area in Figure 15 illustrates the ideal range for each parameter. When evaluating a compound's parameters, the radar plot must align within the pink area to be classified as drug-like. Thus, the radar plot predicts whether the ligands are likely to be orally bioavailable or not. Polarity (POLAR) and Flexibility (FLEX) are two crucial properties that play a significant role in determining the bioavailability of compounds. FLEX is established by rotatable bonds; molecules with more than 10 rotatable bonds are predicted to have low oral bioavailability. The topological polar surface area (TPSA) determines polarity,⁴⁵ indicating that compounds with a TPSA exceeding 20 Å² but less than 130 Å² exhibit high oral bioavailability.^{37,44}

In comparison to other compounds, Ferulic acid stands out as it meets the radar plot criteria, suggesting potential oral bioavailability. Vitexin, with a TPSA of 181.05, is also considered to exhibit high oral bioavailability, while beta-carotene has a TPSA of 0.00. When Tamoxifen was included as a reference ligand, its radar plot showed that most of its physicochemical properties fall within or close to the optimal range, particularly in terms of lipophilicity (LIPO), size, and flexibility (FLEX). However, its polarity lies outside the ideal pink area, suggesting a relatively low TPSA. This indicates lower polarity, which may affect water solubility but not necessarily oral bioavailability. Overall, Tamoxifen exhibits an acceptable bioavailability profile, reinforcing its established use as an orally administered drug.

Table 7. Predicted lipophilicity and physicochemical variables of selected compounds generated using a SwissADME server

Properties	Parameters	Vitexin	Beta-carotene	Ferulic acid	Tamoxifen
Physicochemical Properties	MW (g/mol)	432.38	536.87	194.18	371.51
	Rotatable bonds	3	10	3	8
	HBA	10	0	4	2
	HBD	7	0	2	0
	Fraction Csp3	0.29	0.45	0.10	0.23
Lipophilicity Log Po/w	TPSA	181.05	0	66.76	12.47
	iLOGP	1.38	7.79	1.62	4.64
	XLOGP3	0.21	13.54	1.51	7.14
	MLOGP	-2.02	8.96	1.00	5.10
	Consensus	-0.07	11.11	1.36	5.77

MW = Molecular weight, TPSA = Topological polar surface area, HBA = hydrogen bound acceptor, HBD = hydrogen bound donor.

Table 8. Predicted pharmacokinetics parameters of selected compounds by pkCSM server

Properties	Parameters	Vitexin	Beta-carotene	Ferulic acid	Tamoxifen
Absorption	Water solubility	-2.845	-7.39	-2.817	-5.929
	GI Intestinal absorption (human)	46.695	91.732	93.685	96.885
	Log Kp (skin permeation) cm/s	-2.735	-2.741	-2.72	-2.737
Distribution	BBB	-1.449	0.938	-0.239	1.329
	CNS permeation (Log PS)	-3.834	-1.094	-2.612	-1.473
	VD (human)	1.071	0.266	-1.367	0.83
Metabolism CYP2D6	CYP1A2 inhibitor	**	**	**	*
	CYP2C9 inhibitor	**	**	**	**
	CYP2C19 inhibitor	**	**	**	**
	CYP3A4 inhibitor	**	**	**	**
	CYP2D6 inhibitor	**	**	**	*
Excretion	Total Clearance (CL) (log mL/min/kg)	0.444	1.061	0.623	0.556
	Renal OCT2 substrate	**	**	**	**

* = YES, ** = NO effect, OCT2 = organic cation transporter 2, VD = Volume of distribution, BBB = Blood-brain barrier, VDss = steady state volume of distribution, GI = Gastrointestinal, CL = Range: 5mL/min/kg < CL < 15mL/min/kg: >15 mL/min/kg: high; moderate; <5 mL/min/kg: low. logBB>0.3 is considered too readily cross the BBB. logBB <-1 are unsuccessfully delivered to the brain. VDss is deemed low if less 0.71 L/kg (log VDss <-0.15) and exalted if over 2.81 L/kg (log VDss > 0.45). CNS permeability with log PS > -2 is considered to penetrate the CNS, while log PS <-3 is reflected as incapable to enter CNS.

The pink area indicates the ideal range for each property: polarity (TPSA: 20–130 Å²), lipophilicity (XLOGP3: -0.7 to +5.0), solubility (log S ≤ 6), size (MW: 150–500 g/mol), saturation (fraction of sp³ hybridization carbons ≥ 0.25), and flexibility (≤ 10 rotatable bonds).

Cardiac Toxicity Analysis

To thoroughly assess the potential toxicity of the identified biomolecules, their ability to inhibit the hERG (human Ether-à-go-go-Related Gene) potassium channel was evaluated using the CardioToxCSM and pred-hERG 5.0 web servers. This analysis aimed to estimate the likelihood of the compounds blocking the hERG channel, a critical factor associated with

cardiac arrhythmias and other cardiovascular risks. The FDA mandates hERG safety testing for all therapeutic candidates due to the strong correlation between hERG inhibition and fatal cardiac side effects.⁴⁶

According to the results summarized in Table 9, Vitexin, Beta-carotene, and Ferulic acid were all predicted as non-blockers, indicating a low risk of cardiac toxicity with high confidence scores of 91.81%, 99.38%, and 97.58%, respectively. In contrast, Tamoxifen was identified as a hERG blocker with a confidence level of 83.52%, suggesting a potential for cardiac toxicity. This finding aligns with existing pharmacological data, reinforcing the importance of cautious evaluation when repurposing known drugs.

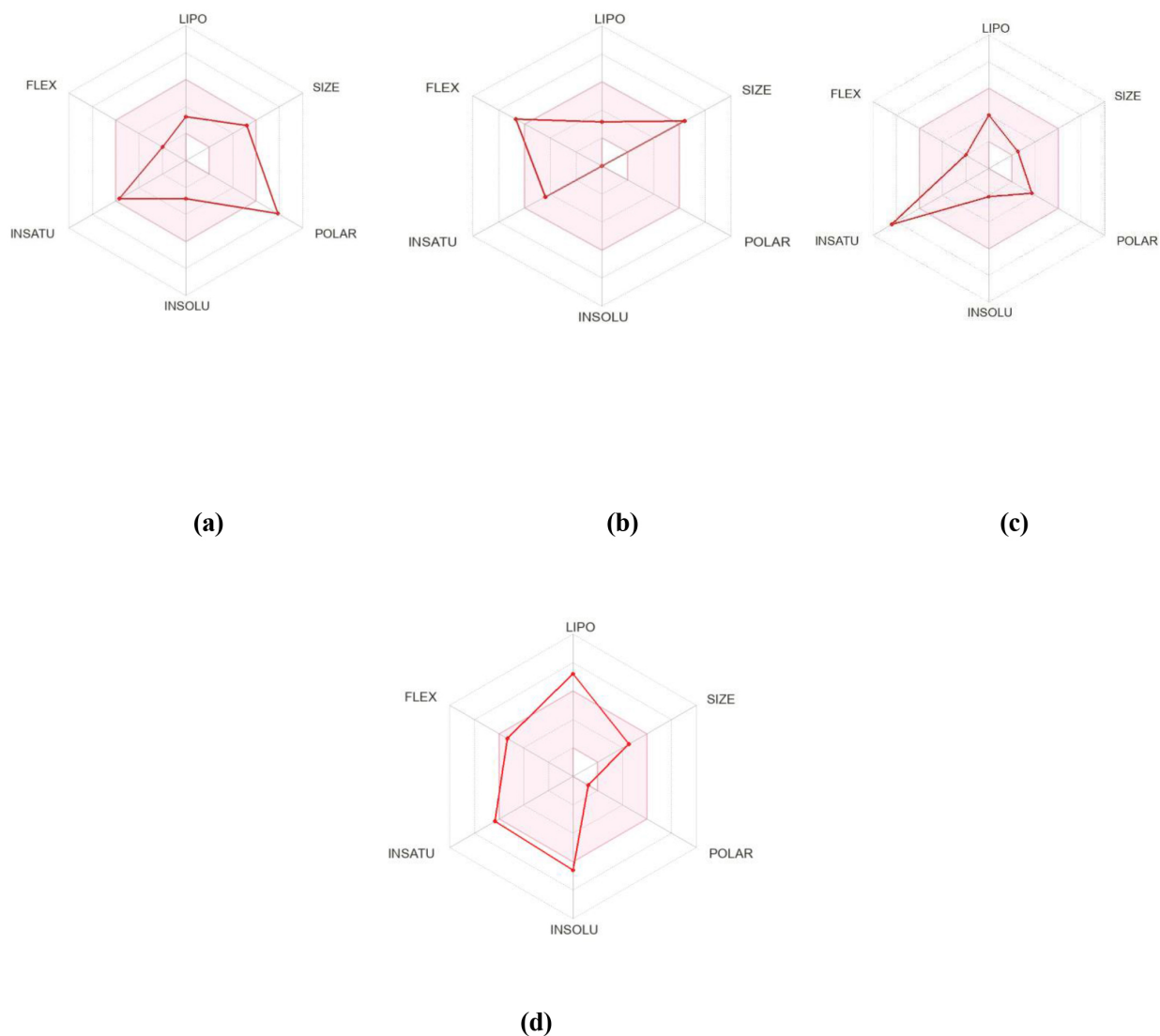


Fig. 15 Radar plots of different ligands: (a) vitexin, which is predicted to be not orally bioavailable due to being too polar; (b) beta-carotene, which is predicted to be not orally bioavailable due to being too flexible; (c) ferulic acid, which is predicted to be orally bioavailable; (d) tamoxifen, which shows a favorable bioavailability profile with most parameters falling within the optimal range, although its low polarity slightly deviates from the ideal zone.

In addition, six key clinical cardiac toxicity outcomes were analyzed to evaluate the safety profiles of the selected compounds, as presented in Table 10. Ferulic acid demonstrated the most favorable profile, showing no signs of toxicity across all indicators, including arrhythmia, cardiac failure, heart block, hERG toxicity, hypertension, and myocardial infarction. In contrast, Vitexin showed toxicity in hERG inhibition and myocardial infarction, suggesting potential cardiovascular concerns. Beta-carotene was also predicted to be toxic in terms of hERG toxicity and hypertension. Tamoxifen exhibited the highest level of cardiac risk, being toxic in four out of six parameters, particularly arrhythmia and myocardial infarction. These findings highlight Ferulic acid's relative cardiac safety and emphasize the need for careful consideration when evaluating compounds like Tamoxifen.

Prediction of Cell Line Cytotoxicity

In-silico predictions were conducted to assess the cytotoxic potential of selected secondary metabolites against various

cancer cell lines, using their Pa (probability of activity) and Pi (probability of inactivity) values. A Pa value greater than 0.5 was considered significant, indicating a potential cytotoxic effect. As presented in Table 11, all tested compounds showed promising cytotoxic activity, with Pa values notably higher than their corresponding Pi values. Beta-carotene exhibited the highest Pa score of 0.889 against the prostate carcinoma cell line (PC-3), suggesting a strong potential for anticancer activity. It also showed moderate cytotoxic potential against the U-266 myeloma cell line. Ferulic acid demonstrated activity against erythroleukemia (K562) and ovarian adenocarcinoma (IGROV-1), with Pa values of 0.542 and 0.529, respectively. Vitexin displayed its highest Pa value (0.696) against the HL-60 promyeloblast leukemia cell line, indicating notable activity in hematopoietic cancers. Notably, Tamoxifen showed strong cytotoxic potential, with a Pa value of 0.811 against the breast carcinoma cell line (MCF7) and 0.573 against ovarian carcinoma (SK-OV-3), supporting its known therapeutic effectiveness in hormone-related cancers. These

Table 9. Assessment of cardiac toxicity in the detected biometabolites employing the pred-hERG 5.0 Webserver

Metabolite Name	Activity on hERG channel	Confiability %
Vitexin	Non-blocker	91.81
Beta-carotene	Non-blocker	99.38
Ferulic acid	Non-blocker	97.58
Tamoxifen	Blocker	83.52

Table 10. Assessment of cardiac toxicity in the detected biometabolites employing the cardioToxCSM Webserver

Metabolite	Cardiac toxicity signs					
	Arrhythmia	Cardiac failure	Heart block	hERG toxicity	Hypertension	Myocardial infarction
Vitexin	S	S	S	T	S	T
Beta-carotene	S	S	S	T	T	S
Ferulic acid	S	S	S	S	S	S
Tamoxifen	T	S	S	T	T	T

S = Safe; T = Toxic.

Table 11. In silico prediction of cell line cytotoxicity for secondary metabolite by CLC-pred 2.0

Metabolite Name	Cell line	Cell line full name	Tissue	Tumor type	Pa	Pi
Vitexin	HL-60	Promyeloblast leukemia	Hematopoietic and lymphoid tissue	Leukemia	0.696	0.009
Beta-carotene	PC-3	Prostate carcinoma	Prostate	Carcinoma	0.889	0.004
Ferulic acid	U-266	Plasma cell myeloma	Blood	Myeloma	0.533	0.005
	K562	Erythroleukemia	Hematopoietic and lymphoid tissue	Leukemia	0.542	0.020
Tamoxifen	IGROV-1	Ovarian adenocarcinoma	Ovary	Adenocarcinoma	0.529	0.016
	MCF7	Breast carcinoma	Breast	Carcinoma	0.811	0.010
	SK-OV-3	Ovarian carcinoma	Ovarian	Carcinoma	0.573	0.014

Pa > 0.3, Pi: probability to be inactive; Pa: probability to be active.

results suggest the potential of the studied biomolecules—particularly Beta-carotene, Ferulic acid, and Tamoxifen—as promising candidates for targeting various cancer types through selective cytotoxicity.

In recent years, there has been an increasing interest in investigating natural compounds for their potential bioactive properties in combating various diseases, particularly cancer. *Aspergillus* sp has emerged as a significant source of biologically active metabolites with diverse beneficial effects, containing anti-inflammatory, antiviral, antimicrobial, and anticancer actions.⁴⁷ Several studies have emphasized the valuable role of *Aspergillus* sp as a source of novel bioactive natural products with antiproliferative activity against several cancer cells.⁴⁸ Notably, in our in-silico studies, we identified three secondary metabolites - vitexin, beta-carotene, and ferulic acid - derived from *Aspergillus* sp, which exhibited promising anticancer properties against human cancer cells.¹⁹ Our in-silico analysis revealed that these secondary metabolites demonstrated notable binding energies against key cancer-related proteins, including BRCA1, BRCA2, and TP53. Specifically, vitexin displayed the highest binding energy with all three target proteins, indicating its strong potential as an anticancer agent. Before clinical trials or production, it is essential to assess the toxicological profile of potential medicines. According to

RO5 analysis, ferulic acid met all five criteria, indicating its favorable drug-like properties. While beta-carotene did not fully satisfy the criteria, vitexin showed a deviation in at most one criterion, which is still considered acceptable. Moreover, our analysis suggested that ferulic acid is likely orally bioavailable, further emphasizing its promise as an anticancer compound. The findings indicated that vitexin, beta-carotene, and ferulic acid demonstrated significant activity in terms of cell line cytotoxicity, with Beta-carotene showing high scores for the Prostate cell line (PC-3). Importantly, none of the three selected metabolites exhibited signs of cardiac toxicity. In line with our findings, a study by Zhou et al.⁴⁹ reported the anti-apoptotic effect of vitexin in various cell lines, including breast, ovarian, and prostate, further supporting the potential of vitexin as an anti-cancer agent. Additionally, research by Najafipour et al.⁵⁰ highlighted vitexin's induction of apoptosis in MCF-7 Breast Cancer Cells through the regulation of specific miRNAs expression, corroborating our in-silico results and previous research on vitexin's potential for anticancer therapy. In conclusion, our in-silico analysis, coupled with existing research, underscores the promising future of vitexin as a potential anti-cancer drug, further supporting its development as a valuable addition to anticancer therapy.^{51,52}

Conclusion

Fungal-derived natural products have a wide range of biological activities, making them a valuable alternative to synthetic compounds. In a previous study, highly effective compounds with potential anticancer properties were identified in the fungus *A. flavus*. In this present study, we selected three potent compounds and evaluated their effects on three tumor suppressor proteins in order to find a promising drug candidate for breast cancer. We employed computational techniques such as molecular docking, ADME analysis, pharmacological profiling, and cardiac toxicity assessments.

After performing multiple docking experiments, we can conclude that vitexin has potent effects on cancer proteins (BRCA1, BRCA2, and TP53) compared to other compounds. Both vitexin and ferulic acid successfully docked and confirmed the highest binding energy with the BRCA2 protein.

In addition to its strong binding energies towards the targeted proteins, vitexin also demonstrated safety in cardiac and hepatotoxicity assessments, as well as suitable physicochemical and pharmacokinetic properties. Overall, our findings suggest that vitexin, isolated from *A. flavus*, holds promise as a candidate for the development of anticancer drugs, and further experimental exploration is warranted. Furthermore, the comprehensive pharmacological profile provided, which includes ADME assessments and molecular docking results, lays the groundwork for investigating other bioactive compounds in the future, targeting various types of cancers.

Conflict of Interest

None. ■

References

1. R. Al-Kahtani, N. Mahmood, S. Aamir, Z. Anjum, Visualizing breast cancer research trends in KSA: A bibliometric analysis, *Journal of Taibah University Medical Sciences*, 18 (2023) 1472–1479.
2. O.A. Abulkhair, F.M. Al Tahan, S.E. Young, S.M. Musaad, A.-R.M. Jazieh, The first national public breast cancer screening program in Saudi Arabia, *Annals of Saudi Medicine*, 30 (2010) 350–357.
3. I.A. El Hag, R. Katchabeswaran, L.C. Chiedozi, S.M. Kollur, Pattern and incidence of cancer in Northern Saudi Arabia, *Saudi Medical Journal*, 23 (2002) 1210–1213.
4. E.M. Ibrahim, A.A. Zeeneldin, B.B. Sadiq, A.A. Ezzat, The present and the future of breast cancer burden in the Kingdom of Saudi Arabia, *Medical Oncology*, 25 (2008) 387–393.
5. WHO, Saudi Arabia fact sheet. International Agency for Research on Cancer; 2022. Available from: <https://gco.iarc.fr/today/data/factsheets/populations/682-saudi-arabia-factsheets.pdf>. Accessed July 17, 2023, (2023).
6. H. Sung, J. Ferlay, R.L. Siegel, M. Laversanne, I. Soerjomataram, A. Jemal, F. Bray, Global cancer statistics 2020: GLOBOCAN estimates of incidence and mortality worldwide for 36 cancers in 185 countries, *CA: a Cancer Journal for clinicians*, 71 (2021) 209–249.
7. A.-M. Buga, A.O. Docea, C. Albu, R.D. Malin, D.E. Branisteanu, G. Ianos, S.L. Ianos, A. Iordache, D. Calina, Molecular and cellular stratagem of brain metastases associated with melanoma, *Oncology Letters*, 17 (2019) 4170–4175.
8. A.O. Docea, P. Mitrut, D. Grigore, D. Pirici, D.C. Calina, E. Gofita, Immunohistochemical expression of TGF beta (TGF-beta), TGF beta receptor 1 (TGFBR1), and Ki67 in intestinal variant of gastric adenocarcinomas, *Rom J Morphol Embryol*, 53 (2012) 683–692.
9. E. Blondeaux, L. Arecco, K. Punie, R. Graffeo, A. Toss, C. De Angelis, L. Trevisan, G. Buzzatti, S.C. Linn, P. Dubsky, Germline TP53 pathogenic variants and breast cancer: A narrative review, *Cancer treatment reviews*, 114 (2023) 102522.
10. J. Duncan, J. Reeves, T. Cooke, BRCA1 and BRCA2 proteins: roles in health and disease, *Molecular pathology*, 51 (1998) 237.
11. K. Yoshida, Y. Miki, Role of BRCA1 and BRCA2 as regulators of DNA repair, transcription, and cell cycle in response to DNA damage, *Cancer science*, 95 (2004) 866–871.
12. B. Friedenson, The BRCA1/2 pathway prevents hematologic cancers in addition to breast and ovarian cancers, *BMC cancer*, 7 (2007) 1–11.
13. A.R. Venkitaraman, How do mutations affecting the breast cancer genes BRCA1 and BRCA2 cause cancer susceptibility?, *DNA repair*, 81 (2019) 102668.
14. A.G. Arnold, E. Otegbeye, M.H. Fleischut, E.A. Glogowski, B. Siegel, S.R. Boyar, E. Salo-Mullen, K. Amoroso, M. Sheehan, J.L. Berliner, Assessment of individuals with BRCA1 and BRCA2 large rearrangements in high-risk breast and ovarian cancer families, *Breast cancer research and treatment*, 145 (2014) 625–634.
15. A. Butera, I. Amelio, Deciphering the significance of p53 mutant proteins, *Trends in Cell Biology*, (2024).
16. Liu, B., Zhou, H., Tan, L., Siu, K. T. H., & Guan, X. Y. (2024). Exploring treatment options in cancer: tumor treatment strategies. *Signal Transduction and Targeted Therapy*, 9(1), 175.
17. M.E. Abd El-Hack, S. Abdelnour, M. Alagawany, M. Abdo, M.A. Sakr, A.F. Khafaga, S.A. Mahgoub, S.S. Elnesr, M.G. Gebriel, Microalgae in modern cancer therapy: Current Knowledge, *Biomedicine & Pharmacotherapy*, 111 (2019) 42–50.
18. J.-B. Jouda, C.D. Mbazona, P. Sarkar, P.K. Bag, J. Wandji, Anticancer and antibacterial secondary metabolites from the endophytic fungus *Penicillium sp. CAM64* against multi-drug resistant Gram-negative bacteria, *African Health Sciences*, 16 (2016) 734–743.
19. A.K. Kalimuthu, P. Pavada, T. Panneerselvam, E. Babkiewicz, J. Pijanowska, P. Mrówka, G. Rajagopal, V. Deepak, K. Sundar, P. Maszczyk, Cytotoxic potential of bioactive compounds from *Aspergillus flavus*, an endophytic fungus isolated from *Cynodon dactylon*, against breast cancer: Experimental and computational approach, *Molecules*, 27 (2022) 8814.
20. A.S. El-Sayed, R.A. Zayed, A.F. El-Baz, W.M. Ismaeil, Bioprocesses optimization and anticancer activity of camptothecin from *Aspergillus flavus*, an endophyte of in vitro cultured *Astragalus fruticosus*, *Molecular Biology Reports*, 49 (2022) 4349–4364.
21. T.N. Almanaa, G. Rabie, R.M. El-Mekkawy, M.A. Yassin, N. Saleh, N. El-Gazzar, Antioxidant, antimicrobial and antiproliferative activities of fungal metabolite produced by *Aspergillus flavus* on in vitro study, *Food Science and Technology*, 42 (2021) e01421.
22. Pal, S., et al. (2022). Fungal secondary metabolites as potential anticancer agents: Current perspectives and future challenges. *Phytomedicine Plus*, 2(1), 100220. <https://doi.org/10.1016/j.phyplu.2021.100220>
23. K. Raval, T. Ganatra, Basics, types and applications of molecular docking: A review, *IP International Journal of Comprehensive and Advanced Pharmacology*, 7 (2022) 12–16.
24. R. Jakhar, M. Dangi, A. Khichi, A.K. Chhillar, Relevance of molecular docking studies in drug designing, *Current Bioinformatics*, 15 (2020) 270–278.
25. Shukla, T. Tripathi, Molecular dynamics simulation in drug discovery: opportunities and challenges, In: Singh, S.K. (eds), *Innovations and implementations of computer aided drug discovery strategies in rational drug design*, Springer, Singapore, (2021) 295–316.
26. C.A. Lipinski, Lead-and drug-like compounds: the rule-of-five revolution, *Drug discovery today: Technologies*, 1 (2004) 337–341.
27. B. Jayaram, T. Singh, G. Mukherjee, A. Mathur, S. Shekhar, V. Shekhar, Sanjeevini: a freely accessible web-server for target directed lead molecule discovery, *BMC Bioinformatics*, Springer, 2012, pp. 1–13.
28. L.E. Mendie, S. Hemalatha, Molecular docking of phytochemicals targeting GFRs as therapeutic sites for cancer: an in silico study, *Applied Biochemistry and Biotechnology*, 194 (2022) 215–231.
29. A. Muhammad, B.S. Katsayal, G.E. Forcados, I. Malami, I.B. Abubakar, A.I. Kandi, A.M. Idris, S.u. Yusuf, S.M. Musa, N. Monday, In silico predictions on the possible mechanism of action of selected bioactive compounds against breast cancer, *In Silico Pharmacology*, 8 (2020) 1–13.

30. J.I. Vandenberg, M.D. Perry, M.J. Perrin, S.A. Mann, Y. Ke, A.P. Hill, hERG K⁺ channels: structure, function, and clinical significance, *Physiological Reviews*, (2012).
31. H.-M. Lee, M.-S. Yu, S.R. Kazmi, S.Y. Oh, K.-H. Rhee, M.-A. Bae, B.H. Lee, D.-S. Shin, K.-S. Oh, H. Ceong, Computational determination of hERG-related cardiotoxicity of drug candidates, *BMC Bioinformatics*, 20 (2019) 67–73.
32. R. C Braga, V. M Alves, M. FB Silva, E. Muratov, D. Fourches, A. Tropsha, C. H Andrade, Tuning HERG out: antitarget QSAR models for drug development, *Current Topics in Medicinal Chemistry*, 14 (2014) 1399–1415.
33. R.C. Braga, V.M. Alves, M.F. Silva, E. Muratov, D. Fourches, L.M. Lião, A. Tropsha, C.H. Andrade, Pred-hERG: A novel web-accessible computational tool for predicting cardiac toxicity, *Molecular Informatics*, 34 (2015) 698–701.
34. Y. Hu, Q. Ren, X. Liu, L. Gao, L. Xiao, W. Yu, In silico prediction of human organ toxicity via artificial intelligence methods, *Chemical Research in Toxicology*, 36 (2023) 1044–1054.
35. K.A. Majorek, M.D. Zimmerman, M. Grabowski, I.G. Shabalin, H. Zheng, W. Minor, Assessment of crystallographic structure quality and protein–ligand complex structure validation, *Structural Biology in Drug Discovery: Methods, Techniques, and Practices*, (2020) 253–275.
36. A.A. Lagunin, V.I. Dubovskaja, A.V. Rudik, P.V. Pogodin, D.S. Druzhilovskiy, T.A. Glorizova, D.A. Filimonov, N.G. Sastry, V.V. Poroikov, CLC-Pred: A freely available webservice for in silico prediction of human cell line cytotoxicity for drug-like compounds, *PLoS One*, 13 (2018) e0191838.
37. D. Ji, M. Xu, C.C. Udenigwe, D. Agyei, Physicochemical characterisation, molecular docking, and drug-likeness evaluation of hypotensive peptides encrypted in flaxseed proteome, *Current Research in Food Science*, 3 (2020) 41–50.
38. G.B. Khan, M. Qasim, A. Rasul, U.A. Ashfaq, A.M. Alnuqaydan, Identification of lignan compounds as new 6-phosphogluconate dehydrogenase inhibitors for lung cancer, *Metabolites*, 13 (2022) 34.
39. T.M. Fakhri, D.S.F. Ramadhan, F. Darusman, In silico activity identification of cyclo peptide alkaloids from *Zizyphus spina-christi* species against Sars-Cov-2 main protease, *Jurnal Biodjati*, 6 (2021) 71–81.
40. P. Chinnasamy, R. Arumugam, In silico prediction of anticarcinogenic bioactivities of traditional anti-inflammatory plants used by tribal healers in Sathyamangalam wildlife Sanctuary, India, *Egyptian Journal of Basic and Applied Sciences*, 5 (2018) 265–279.
41. B.E. Oyinloye, T.A. Adekiya, R.T. Aruleba, O.A. Ojo, B.O. Ajiboye, Structure-based docking studies of GLUT4 towards exploring selected phytochemicals from *Solanum xanthocarpum* as a therapeutic target for the treatment of cancer, *Current drug discovery technologies*, 16 (2019) 406–416.
42. J. Suganya, M. Radha, D.L. Naorem, M. Nishandhini, In silico docking studies of selected flavonoids-natural healing agents against breast cancer, *Asian Pacific Journal of Cancer Prevention*, 15 (2014) 8155–8159.
43. Y. Han, J. Zhang, C.Q. Hu, X. Zhang, B. Ma, P. Zhang, In silico ADME and toxicity prediction of ceftazidime and its impurities, *Frontiers in Pharmacology*, 10 (2019) 434.
44. A. Daina, O. Michielin, V. Zoete, SwissADME: a free web tool to evaluate pharmacokinetics, drug-likeness and medicinal chemistry friendliness of small molecules, *Scientific Reports*, 7 (2017) 42717.
45. M.R. Xavier, M.M. Marinho, M.S. Julião, E.S. Marinho, F.W. Almeida-Neto, K.K. de Castro, J.P. da Hora, M.N. da Rocha, A.C. Barreto, G.D. Saraiva, Structural, topological, vibrational, and electronic analysis, and ADMET study of methyl-2-(4-isobutylphenyl) propanoate, *Journal of Molecular Structure*, 1309 (2024) 138019.
46. S.S.U. Hassan, S.Q. Abbas, F. Ali, M. Ishaq, I. Bano, M. Hassan, H.-Z. Jin, S.G. Bungau, A Comprehensive in silico exploration of pharmacological properties, bioactivities, molecular docking, and anticancer potential of vieloplain F from *Xylopiella vielana* Targeting B-Raf Kinase, *Molecules*, 27 (2022) 917.
47. I. Bhatnagar, S.-K. Kim, Immense essence of excellence: marine microbial bioactive compounds, *Marine Drugs*, 8 (2010) 2673–2701.
48. S. Sinha, S. Das, B. Saha, D. Paul, B. Basu, Anti-microbial, anti-oxidant, and anti-breast cancer properties unraveled in yeast carotenoids produced via cost-effective fermentation technique utilizing waste hydrolysate, *Frontiers in Microbiology*, 13 (2023) 1088477.
49. Y. Zhou, Y.E. Liu, J. Cao, G. Zeng, C. Shen, Y. Li, M. Zhou, Y. Chen, W. Pu, L. Potters, Vitexins, nature-derived lignan compounds, induce apoptosis and suppress tumor growth, *Clinical Cancer Research*, 15 (2009) 5161–5169.
50. R. Najafipour, A.M. Momeni, Y. Mirmazloomi, S. Moghbelinejad, Vitexin induces apoptosis in MCF-7 breast cancer cells through the regulation of specific miRNAs expression, *International Journal of Molecular and Cellular Medicine*, 11 (2022) 197.
51. Rashwan, A. K., Younis, H. A., Abdelshafy, A. M., Osman, A. I., Eletmany, M. R., Hafouda, M. A., & Chen, W. (2024). Plant starch extraction, modification, and green applications: a review. *Environmental Chemistry Letters*, 1–48. <https://doi.org/10.1007/s10311-024-01753-z>
52. Elzagheer, M. A., Wadea, M. K., Ali, N. M., & Eletmany, M. R. (2024). Enhancing Antioxidant Status, Productive and Reproductive Performance for Post-Molt Broiler Breeders by Using Maca Powder (*Lepidium Meyenii*). *Chelonian Conservation and Biology*, 19(01), 485–499.

This work is licensed under a Creative Commons Attribution-NonCommercial 3.0 Unported License which allows users to read, copy, distribute and make derivative works for non-commercial purposes from the material, as long as the author of the original work is cited properly.